ACS OMEGA

http://pubs.acs.org/journal/acsodf

Article

In Situ Preparation of High-Performance Silicon-Based Integrated Electrodes Using Cross-Linked Cyclodextrins

Hao-wen Jiang,[§] Yu Qin,[§] Yi-ming Nie, Zhi-fang Su, Yun-fei Long, Yanxuan Wen, and Jing Su*

Cite This: *ACS Omega* 2023, 8, 5683−5691

Read Online

ACCESS | Metrics & More | Article Recommendations | Supporting Information

ABSTRACT: The strategy of material modification for improving the stability of silicon electrodes is laborious and costly, while the conventional binders cannot withstand the repeated massive volume variability of silicon-based materials. Hence, there is a demand to settle the silicon-based materials' problems with green and straightforward solutions. This paper presents a high-performance silicon anode with a binder obtained by in situ thermal cross-linking of citric acid (CA) and β-cyclodextrin (β-CD) during the electrode preparation process. The Si electrode with a binder synthesized by the one-pot method shows excellent cycling performance. It maintains a specific capacity of 1696 mAh·g^{-1} after 200 cycles at a high current of 0.5 C. Furthermore, the carbonylation of β-CD to carbonyl-β-CD (c-β-CD) introduced better water solubility, and the c-β-CD can generate multidimensional connections with CA and Si, which significantly enhances the specific capacity to 1941 mAh·g^{-1} at 0.5 C. The results demonstrate that the prepared integrated electrode facilitates the formation of a stable and controllable solid electrolyte interface layer of Si and accommodates Si's repeated giant volume variations.

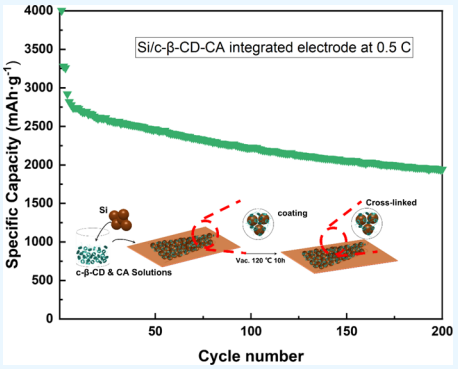

1. INTRODUCTION

Lithium-ion batteries, potassium-ion batteries, and so on have attracted extensive attention due to their high energy density and low cost. However, they all face the same challenge, that is, how to further improve the energy density and battery stability.[1,2]

In the field of lithium-ion batteries, the abundant and cost-effective silicon-based material with a theoretical specific capacity of nearly 4200 mAh·g^{-1}, as one of the most promising anode materials, can greatly improve the energy density.[2] However, this material has a dramatic volume change (300%) during charge/discharge and is accompanied by challenging problems, such as electrolyte decomposition and solid electrolyte interface (SEI) film destabilization caused by the electrode cracking. All of the above issues lead to a rapid capacity degradation and shortened cycle lifetime, limiting the application of silicon in Li-ion batteries.[3] In addition to developing advanced electrolytes to form a stable anodic passivation layer, there are also two main strategies to improve the cycling stability of silicon anodes: the modification of the active substance itself and the adoption of a binder with healing ability.[3,4] The latter utilizes an elastic binder to relieve the stress of silicon during the charging and discharging process, making it a highly desirable solution.[5]

The binder in lithium-ion batteries is a polymer that enhances the connection between the active mass and the conductive material, which binds the active mass to the current collector.[6,7] The polymer binder widely commercially available is mainly polyvinylidene fluoride (PVDF). However, the weak van der Waals forces between Si and PVDF cannot accommodate Si's drastic volume changes and require the use of a toxic and expensive organic dispersant (*N*-methyl-2-pyrrolidone).[8−10] The cycle performance of the modified Si/PVDF electrode, on the other hand, was considered to be improved and yet still unsatisfactory.[8−10] Various low-cost, simple-to-prepare aqueous adhesives have been investigated.[11,12] Polymers such as chitosan (CS),[13] carboxymethyl cellulose salt (CMC),[14] polyacrylic acid (PAA),[15] and sodium alginate[16] are plentiful in polar groups, which can form hydrogen bonds and chemical bonds with silicon. The binders have stronger adhesion to silicon electrodes. These binders exhibit favorable adhesion and potential self-healing function in the industrial production of batteries. In addition, composite binders cross-linked with other binders or modified by metal ions, such as Li$_x$PAA,[17] PFA-TPU,[18] etc., also have significant achievements in enhancing the performance of silicon-based negative electrodes. In the study of Wu et al., "Hard" poly(furfuryl alcohol) (PFA) and "soft" thermoplastic polyurethane (TPU) are interweaved into 3D conformation to confine SiO$_x$ particles via in situ polymerization.[18] Choi et al.[19]

Received: November 7, 2022
Accepted: January 20, 2023
Published: February 2, 2023

connected α-cyclodextrin, polyvinyl alcohol, and PAA to form a mechanical sliding interlocking molecular pulley model. They found that the steric structure of the cross-linked binder not only kept the structural integrity of the silicon anode but also strengthened the electrochemical performance to a certain extent. Some research has suggested that composite binders with a three-dimensional network structure can further boost the bonding force between the binder and the active material and provide a solid mechanical support for the electrode.[20,21] Nevertheless, improving the electrochemical performance of silicon anodes by the binders mentioned above is not sufficient to achieve long-term durability because of the loss of electrode integrity, which is caused by the insufficient mechanical strength of the binder and the weak connection between the silicon and the binder.

β-Cyclodextrin (β-CD) is an oligosaccharide containing seven D(+)-glucose molecules linked to form a conical, circular structure. β-CD includes seven primary hydroxyl groups and 14 secondary hydroxyl groups at the two ports, which can react with other functional groups for chemical modification.[22] Given the unique cavity structure and abundant hydroxyl groups, β-CD can be combined with cross-linking materials to form a mesh structure. The reported effective cross-linking chemicals are epichlorohydrin,[23] citric acid (CA),[24] EDTA,[25] etc. Recently, many researchers have discovered that β-CD is also a suitable choice for the binder of lithium-ion batteries. Jeong et al.[23] introduced hyperbranched β-cyclodextrin (β-CDp) as a novel silicon anode binder in 2014, and produced a β-CDp/alginate (Alg) binder by fully optimizing the mass ratio. Then, it was shown that when β-CDp accounted for 87%, the specific capacity of the electrode remained 70.6% after 100 cycles. This β-CDp hyperbranched network structure exhibits a powerful bonding effect by multidimensional hydrogen bonding. The Si particles are less susceptible to detachment and exhibit better cycling performance.

In the present study, we developed a better binder for silicon anodes by optimizing electrode preparation. Inspired by previous research on three-dimensional network binders from the traditional Chinese cuisine of glutinous rice, researchers have indicated that the abundant branched polysaccharides and the numerous carboxyl groups in glutinous rice make it possess powerful bonding properties. In the past studies, glutinous rice has been utilized to restore the historic city walls, giving them better toughness through hydrogen bonding.[26] Motivated by the advanced processing of β-CD, a further product of starch, we designed and prepared silicon-based integrated electrodes with a simple process. In electrode fabrication, the environmentally friendly CA was cross-linked with β-CD. However, the poor water solubility of β-CD leads to many additional challenges for electrode production. A carbonylation reaction for β-CD was proceeded to improve the solubility and promote the esterification with CA. It enables the introduced carboxyl groups to form lipid-like bonds with the functional groups on the silicon surface, enhancing the resistance of the integrated electrode to stress changes.

2. EXPERIMENTAL SECTION

2.1. Preparation of Electrodes. The integrated electrode preparation procedure is shown in Figure 1a. A percentage of β-CD (Tianjin Damao Chemical Reagent Factory) and CA (Aladdin Reagent Co.) was weighed and dissolved in potassium dihydrogen phosphate to yield a mixed binder solution. The commercial nano-Si (100 nm, Shanghai ST-NANO Science & Technology Co.), conductive carbon black, and binder were sufficient milled in an agate mortar according to the mass ratio of 6:2:2. The weight of the binder is the sum of the masses of β-CD and CA. A homogeneous slurry was acquired by thorough mixing using a high-speed oscillating ball mill. Then, the slurry was coated uniformly on the copper foil with a squeegee, and the spacing gap between the squeegee and the copper foil was 90 μm during the coating operation. The electrode films were achieved by predrying in an oven at 60 °C for 6 h followed by overnight drying under vacuum at 120 °C to evaporate the solvent completely. The electrodes were punched into disks (14 mm in diameter) for cell assembly and electrochemical testing. The β-CD was oxidized by hydrogen peroxide, as described in Figure 1b. The electrode preparation process was repeated unless the β-CD was replaced by c-β-CD.[27]

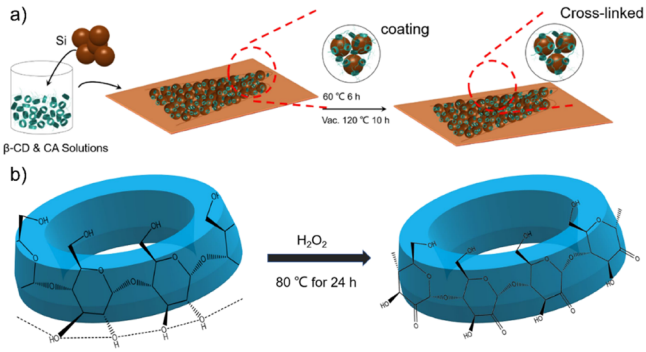

Figure 1. (a) Electrode preparation process. (b) Carbonylation modification of β-CD.

2.2. Material Characterization. Scanning electron microscopy (SEM) was adopted to observe the surface of electrode poles before and after cycling. A Bruker D8 Advance X-ray diffractometer from Germany was utilized to test the samples. The test conditions included Cu-Kα rays at a wavelength of 1.5406 Å, a tube current of 40 mA, a tube pressure at 40 kV, with a scan rate of 20 °/min, and a 2θ scan range from 10 to 80°. The binder's chemical composition and functional groups were determined by Fourier transform infrared spectroscopy (FTIR) in the range of 4000−500 cm^{-1}. The ramp-up rate for thermogravimetric analysis was 10 °C·min^{-1}, from room temperature to 600 °C.

2.3. Electrochemical Test. We fabricated CR2032 coin cells in a glovebox (Ar gas atmosphere) adopting the Si-based integrated working electrode and lithium metal as the counter and reference electrode, which were separated by a polypropylene membrane (Celgard 2400). Herein, battery-grade fluorosubstituted ethylene carbonate and lithium hexafluorophosphate solution (1 M $LiPF_6$ in EC/DEC = 50/50 (v/v)) were used as the electrolyte. Galvanostatic tests for the cells were tested on a Neware cell tester between 0.01 and 1.5 V at 25 °C. The cell was activated at 0.1 C for three cycles before cycling at 0.5 C. The theoretical capacity of Si was calculated at 4200 mAh·g^{-1}. Cyclic voltammetry (CV) data were acquired at a scan rate of 0.1 mV·s^{-1} by a Gamry Interface 1010E electrochemical workstation, USA. The electrochemical impedance spectroscopy (EIS) testing frequency was 0.1 Hz−100 kHz, and the AC amplitude was 5 mV.

https://doi.org/10.1021/acsomega.2c07182
ACS Omega 2023, 8, 5683−5691

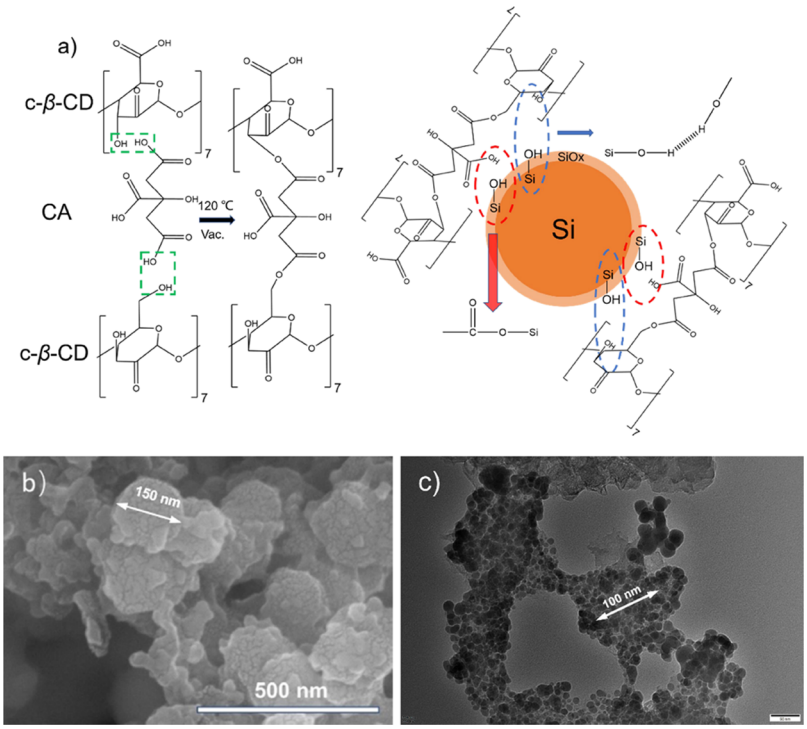

Figure 2. (a) Mechanism of action of the Si/c-β-CD-CA electrode, (b) SEM image of the Si/c-β-CD-CA electrode, (c) transmission electron microscopy image of the Si/c-β-CD-CA electrode after 50 cycles.

3. RESULTS AND DISCUSSION

3.1. Characterization of Cross-Linked Materials.

Figure 2a,b schematically illustrates the mechanism of action of this 3D network binder. In the mixing process, the c-β-CD and CA are wrapped on the surface of Si particles. Under the effect of high temperature, the hydroxyl group of c-β-CD undergoes esterification with the carboxyl group of CA to generate a mesh structure polymer, which coats the Si particles with a protective layer, as shown in Figure 2a. The particle size of silicon particles marked in Figure 2b is 150 nm, which is larger than their original particle size. This proves the existence of the protective layer constructed by the adhesive. The carbonyl group in c-β-CD promotes the esterification of hydroxy l groups to form c-β-CD-CA. Similar to conventional CMC and PAA, a substantial quantity of reactive carboxyl groups form lipid-like bonds with Si−OH on the Si surface, as shown in the red circles in Figure 2a. The abundant hydroxyl groups on c-β-CD can also constitute multidimensional hydrogen bonds with Si as the blue circle in Figure 2a. Even though the volume of Si expands during Si lithiation, the linear CA molecules are cross-linked with c-β-CD to form a mesh structure that disperses the significant stresses, avoiding the separation of the active material, collector, and conductive carbon black. Figure 2c shows that silicon particles are covered by a large amount of conductive carbon black without being exposed after 50 cycles. It confirms that the protective layer composed of adhesive can effectively prevent the breakage of silicon particles. However, in the process of de-lithiation, the volume of the active material decreases, while CA remains attached to the surface of the Si particles due to covalent bonding, thereby effectively preventing the SEI layer from being generated again.[28]

To determine the bonding of the cross-linked binder, β-CD (or c-β-CD) and CA were dissolved in a potassium dihydrogen phosphate solution. Subsequently, the mixture was predried in an oven at 60 °C for 6 h and dried overnight under vacuum at 120 °C to altogether remove the solvent. The FTIR test results are shown in Figure 3. In the spectrum of CA, the peak at

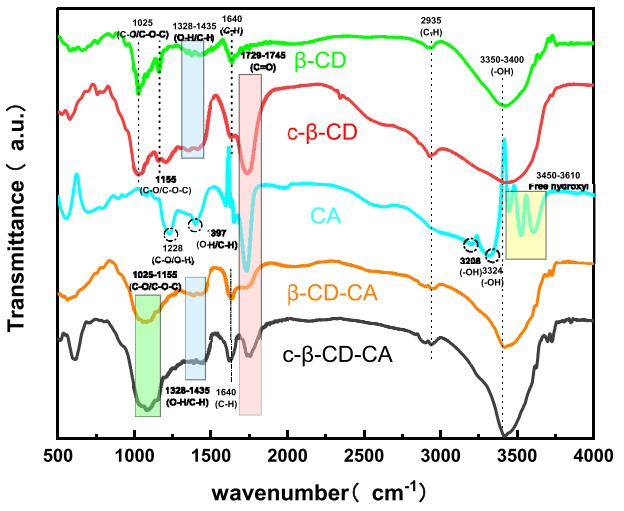

Figure 3. FTIR spectra of individual binders.

about 1729 cm^{-1} is attributed to the stretching vibration of the carboxylate C═O. The narrow and sharp peaks of CA in 3450−3610 cm^{-1} are attributed to the free hydroxyl groups (no hydrogen bond is formed), and the absorption peaks at around 3300 cm^{-1} are owing to the hydroxyl group forming hydrogen bonds. In the spectra of other substances containing CA, the disappearance of the free hydroxyl peaks in the range of 3450−3610 cm^{-1} is caused by its participation in esterification or the formation of intermolecular hydrogen bonds due to the introduction of water. The characteristic

https://doi.org/10.1021/acsomega.2c07182
ACS Omega 2023, 8, 5683−5691

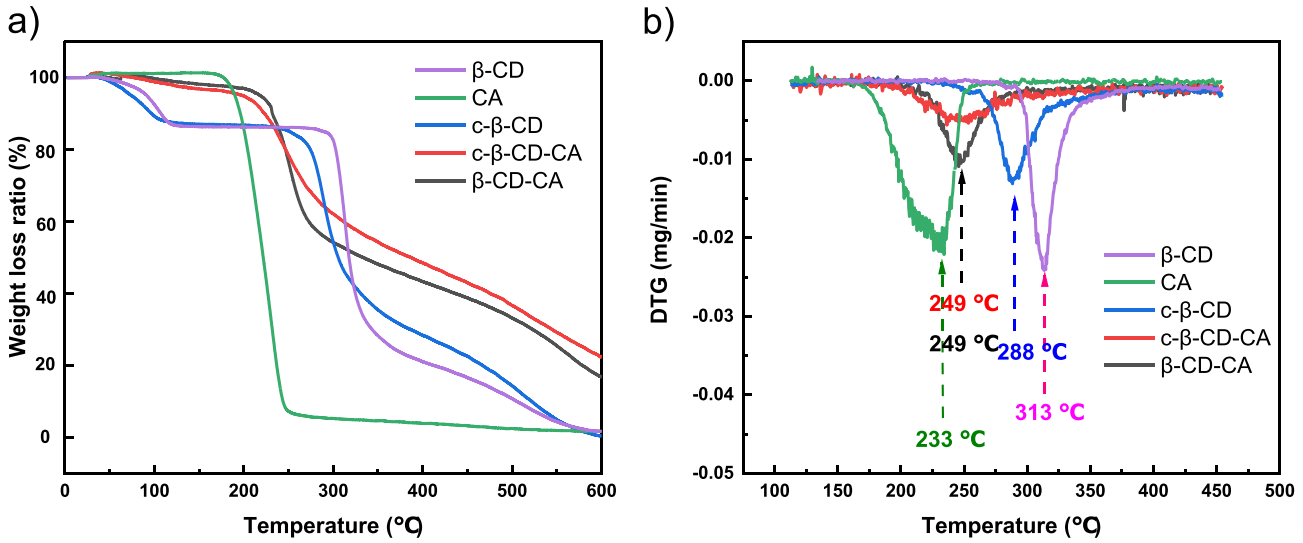

Figure 4. (a) TG curves for individual binders. (b) DTG curves.

absorption peaks of β-CD at 1025 and 1155 cm^{-1} are caused by C−O−C and C−O stretching vibrations in the lumen. The absorption peak at 2935 cm^{-1} is induced by C−H stretching vibrations in the methylene, and the absorption peak at about 3350 cm^{-1} is owing to O−H stretching vibrations. The β-cyclodextrin-citric acid polymer (β-CD-CA) shows a new absorption peak at 1745 cm^{-1} compared to the β-CD monomer, which is caused by the C═O stretching vibration in the ester group. The broadening and blunting bands (C−O−C/C−O) in 1025−1155 cm^{-1} are also the symbols of ester group formation. The change from a single peak to double peaks near 2900 cm^{-1} is attributed to the new C−H bond by the cross-linked CA. These results prove that the hydroxyl groups outside the β-CD of the cavity were successfully esterified, and a reticulated polymer was constituted. Likewise, we perform FTIR tests on the carbonylated sample (c-β-CD). Compared to the untreated β-CD, the c-β-CD has a new peak at 1729 cm^{-1} attributed to the stretching vibration of the carboxylate C═O. Except for this new peak, the FTIR spectrum of c-β-CD shows no other significant variations before and after carbonylation. It suggests that the original ring structure of β-CD was not destroyed during oxidation. According to previous studies,[27] a hydrogen-bonding band external to the lumen of β-CD gives the whole β-CD a robust and rigid structure, resulting in β-CD being insoluble in water at room temperature. After the oxidizing part of extraluminal hydroxyl groups to carboxyl groups, the strong hydrogen bonding network of β-CD is broken, and c-β-CD is preferred to form intermolecular hydrogen bonds, increasing its solubility.

Thermogravimetric analysis (TGA) confirms the presence of cross-linked structures as well. As can be noticed in the TGA results in Figure 4, the TG curves of the cross-linked samples tended similarly to the TG curves of β-CD. The pyrolysis temperature of β-CD itself is 313 °C, and that of CA is 233 °C, whereas that of β-CD-CA/c-β-CD-CA is 249 °C, which is between them. Thus, it is clear that cross-linking changes the pyrolysis temperature of the material.[29]

To detect the interaction between the binder and active particles by X-ray diffraction (XRD), the β-CD-CA or c-β-CD-CA was mixed with Si at 1:1, followed by vacuum drying at 120 °C. As shown in Figure 5, since commercial silicon is applied

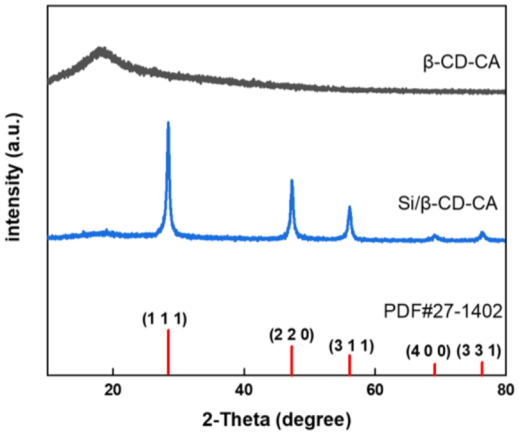

Figure 5. XRD patterns of β-CD-CA and Si/β-CD-CA.

directly without any treatment, usually commercial silicon has a crystalline silicon core and an outside silicon oxide layer.[30] However, the oxide layer is too thin for XRD detection. The plate peak near 20° (2θ) in the XRD pattern is due to the cross-linked binder. All of the sample peaks after mixing β-CD-CA with Si and high-temperature treatment are consistent with the PDF card of Si (PDF#27-1402), suggesting that the introduction of the binder did not alter the physical phase structure of Si.

The FTIR results are shown in Figure 6a. The significant change of the −O−H peak at 3400 cm^{-1} indicates a new hydrogen bond interaction between the binder and Si particles. Meanwhile, because of the presence of hydrogen bonds, the C═O stretching vibration peaks in the original ester groups are all shifted to lower wavenumbers, from 1745 cm^{-1} (Figure 3) to 1716 cm^{-1} and 1739 cm^{-1}, respectively. Furthermore, it is worth noting that the absorption peak around 1700 cm^{-1} splits into two peaks, as shown in the enlarged view in Figure 6b. This is attributed to forming a lipid-like bond between the binder and Si. The presence of these hydrogen and lipid-like bonds can adapt to the enormous volume changes of Si and stabilize the SEI membrane during the cycling process.[28]

We also fold the Si/β-CD-CA and Si/c-β-CD-CA electrodes. As visible in the HD digital camera in Figure 7, a small amount of powder falls out from the center of the β-CD-CA after two

https://doi.org/10.1021/acsomega.2c07182
ACS Omega 2023, 8, 5683−5691

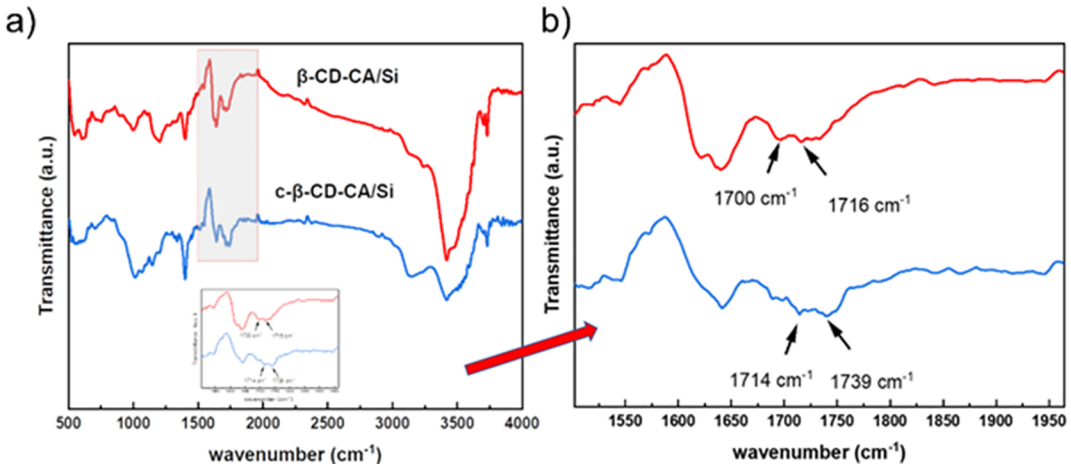

Figure 6. (a) FTIR spectra of Si/β-CD-CA and Si/c-β-CD-CA. (b) Local magnification of FTIR spectra.

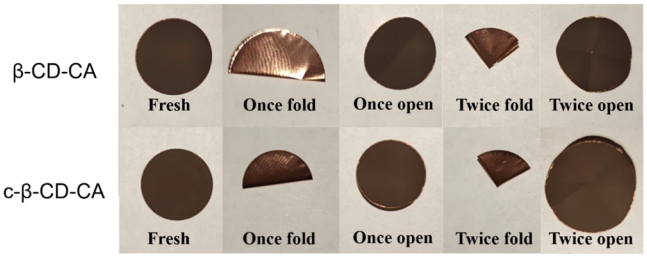

Figure 7. Folded photos of the Si/β-CD-CA electrode sheet and Si/c-β-CD-CA electrode sheet.

foldings, while Si/c-β-CD-CA can still keep the electrode intact after two folds without obvious damage or cracks, further demonstrating the apparent advantage of the c-β-CD-CA binder in mechanical properties. The peel test data of Figure S1 confirmed that the introduction of carbonyl groups has a significant effect on the improvement of the mechanical properties.

3.2. Electrochemical Tests. Figure 8a–c illustrates the CV curves of the Si/β-CD-CA, Si/c-β-CD, and Si/c-β-CD-CA electrodes for the previous four cycles at a scan rate of 0.1 mV·s^{-1}. From the figure, it is clear that all binders have similar electrochemical reaction characteristics. During the embedding of lithium ions, a broad cathodic peak appears at 0.17–0.18 V, which corresponds to the alloying reaction ($Si + xLi^+ + xe^- \rightarrow Li_xSi$). For lithium-ion stripping, two anodic peaks appear near 0.36 and 0.53–0.56 V, corresponding to the de-alloying. These are in accordance with previously published results regarding the typical redox peaks of silicon anodes. The intensity of Si's alloying and de-alloying peaks is growing in CV tests due to the activation of Si nanoparticles, which had been reported in other literature. It is also noteworthy that no significant SEI formation peaks were observed between the first cathodic scans. This phenomenon is explained by the fact that this binder effectively mitigates the formation of an SEI, leading to the peaks being flat and inconspicuous. To explore the electrochemical stability of the binder, β-CD-CA(or c-β-CD-CA) is mixed with acetylene black in a 1:1 homogeneous mixture and tested for CV.[31−33] As presented in Figure S2, the gentle peak around 0.75 V is generated by the lithium-ion embedded in acetylene black. There is no apparent redox peak in the voltage interval of 0–3 V, suggesting that the binder does not react in the above voltage range, which is relatively stable and can be applied as a lithium-ion battery binder.

Figure 8d plots the capacity–voltage curves of the first charge and discharge of the two electrodes of β-CD-CA/c-β-CD-CA. The initial reversible capacities of the Si/β-CD-CA and Si/c-β-CD-CA electrodes in the potential range of 0.01–1 V are 3279 and 3555 mAh·g^{-1}, respectively, with first-time efficiencies of 83.02 and 84.12%. Such a high CE confirms that the three-dimensional network constructed by the binder can prevent direct contact between the electrolyte and the Si particles to a certain extent, alleviating the formation of a SEI. There is a distinct plateau between 0 and 0.18 V in the first discharge, and this lithiation process corresponds to the peak at 0.17 V in the CV test. The plateau occurs around 0.3–0.4 and 0.55 V in the initial charging process, and this de-lithiation process matches the peaks at 0.36 and 0.55 V in the CV test, respectively.[34]

For the further study of the cycling performance of each electrode, charge and discharge tests are performed on each electrode at a current density of 0.5 C. The loading density of the electrode materials was 0.55–0.60 mg·cm^{-2}. The β-CD without any treatment is included as the reference electrode, and the test results are displayed in Figure 9. All electrodes have a similar trend of capacity decay. This is in line with many previously reported findings on 3D binders. By mixing the active substance Si, binder raw materials, etc. and then cross-linking them in one pot to form the integrated electrode, the action between each component of the binder and the binder is further strengthened, as well as between the binder and the active substance Si. The cycling performance of the whole integrated electrode has been significantly improved, sustaining a high specific capacity of 1696 and 1941 mAh·g^{-1} after 200 cycles. However, the electrode prepared by commercial adhesive PVDF only retains the specific capacity of 45.86 mAh·g^{-1} after 200 cycles. Compared with other literature studies,[35,36] the Si/c-β-CD-CA integrated electrode also has advantages in capacity and cycling stability at a high current density of 0.5 C.

The rate performance of different electrodes is shown in Figure S4. The Si/c-β-CD-CA electrode exhibits high specific capacities of 3393, 2905, 2471, and 1996mAh/g, respectively at corresponding rate. In contrast, the Si/β-CD-CA electrode shows inferior rate performance and delivers little capacity. More importantly, after multiple charge–discharge cycles at

https://doi.org/10.1021/acsomega.2c07182
ACS Omega 2023, 8, 5683−5691

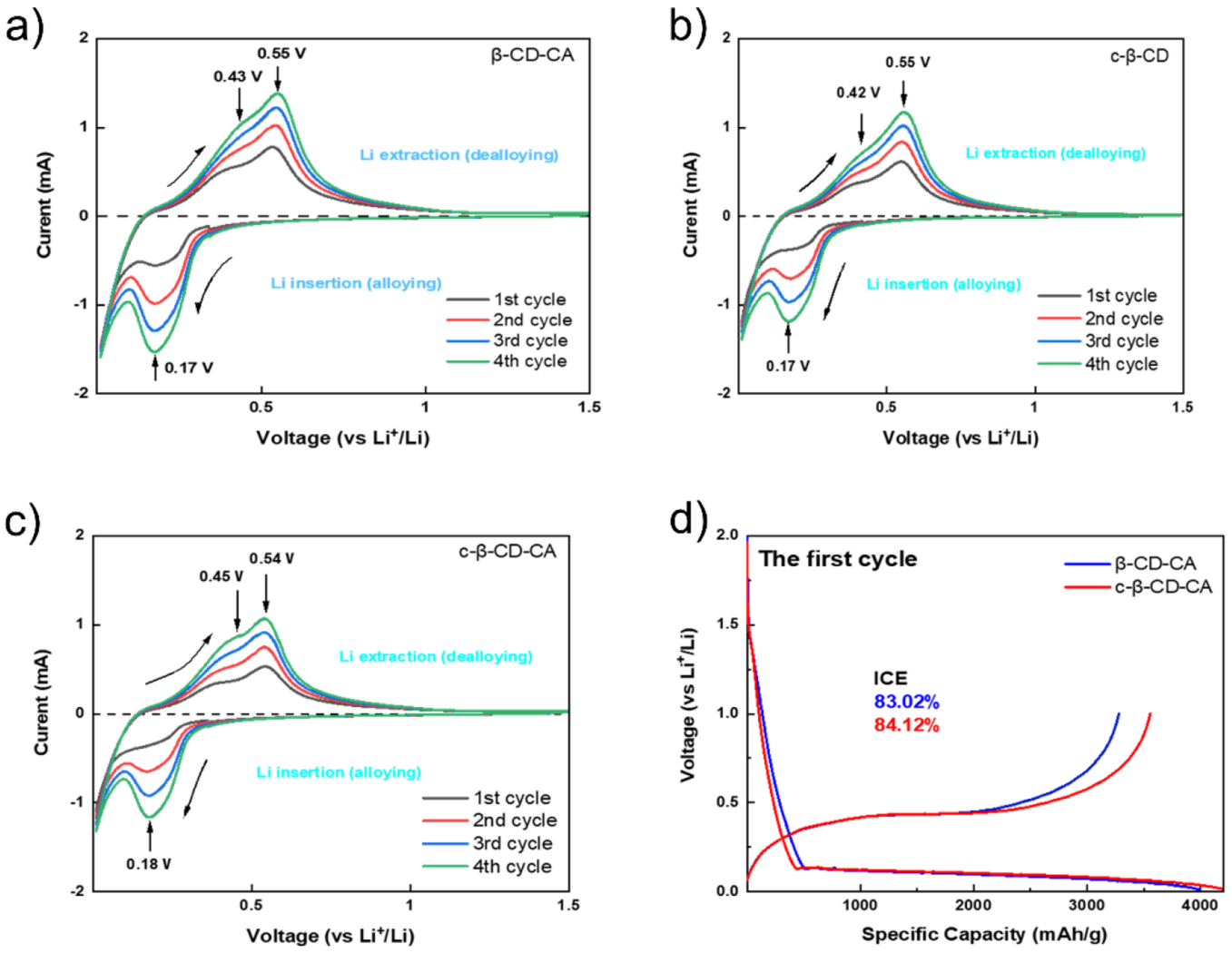

Figure 8. (a) CV curves of Si/β-CD-CA, (b) Si/c-β-CD, and (c) Si/c-β-CD-CA. (d) First charge/discharge curves for Si/β-CD-CA and Si/c-β-CD-CA electrodes.

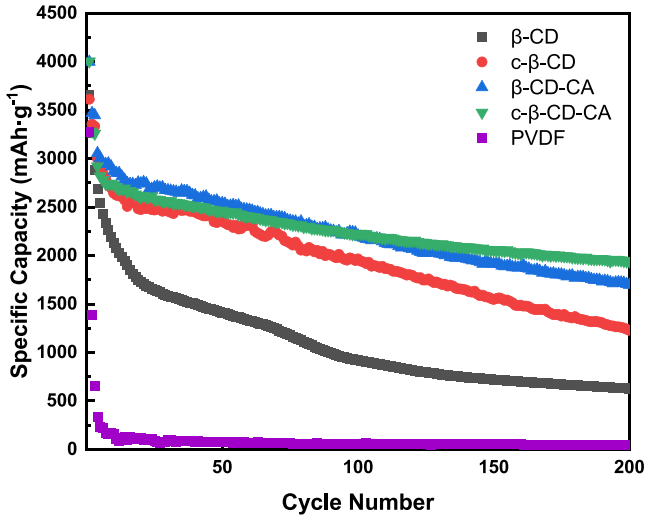

Figure 9. Cycling performance of Si/β-CD, Si/β-CD-CA, Si/c-β-CD, Si/c-β-CD-CA and Si/PVDF at 0.5C.

high current density, a reversible capacity of ~2844 mAh/g was recovered when returning to the initial 0.2 C rate.

3.3. Process and Characteristics of SEI Membrane Formation. To better visualize the changes in the SEI layer of the integrated electrode before and after cycling, we performed EIS tests on the electrode in the fully discharged state after the first cycle and 50 cycles. All data are fitted with the same equivalent circuit. The test and fitting performance is given in Figure 10a,b and Table 1. The Rsei is significantly decreased after 50 cycles. The Si/β-CD-CA electrode had the ability to hold the Rsei at 14.44 Ω. By carbonylating β-CD, the mechanical properties of the integrated electrode are enhanced, and the Rsei is stabilized faster. The Si/c-β-CD-CA electrode retains the Rsei at 7.53 Ω after 50 cycles.

The CR2032 cells were disassembled before and after 50 cycles, and SEM observed the cracks of the pole pieces. From Figure 11a–c, the coatings are uniformly distributed on the copper foil when the charging and discharging are not performed. The Si/c-β-CD electrode in Figure 11e has large cracks after cycling, and the integrity of the electrode is destroyed. With the increase in the quantity of alloying/dealloying, the crashes become more significant, and the coating gradually comes off the collector, causing a rapid drop in capacity. In comparison with the Si/β-CD-CA electrode in Figure 11d,f, the surface of the Si/c-β-CD-CA electrode is flatter and less cracked after cycling. This is facilitated by the

https://doi.org/10.1021/acsomega.2c07182
ACS Omega 2023, 8, 5683−5691

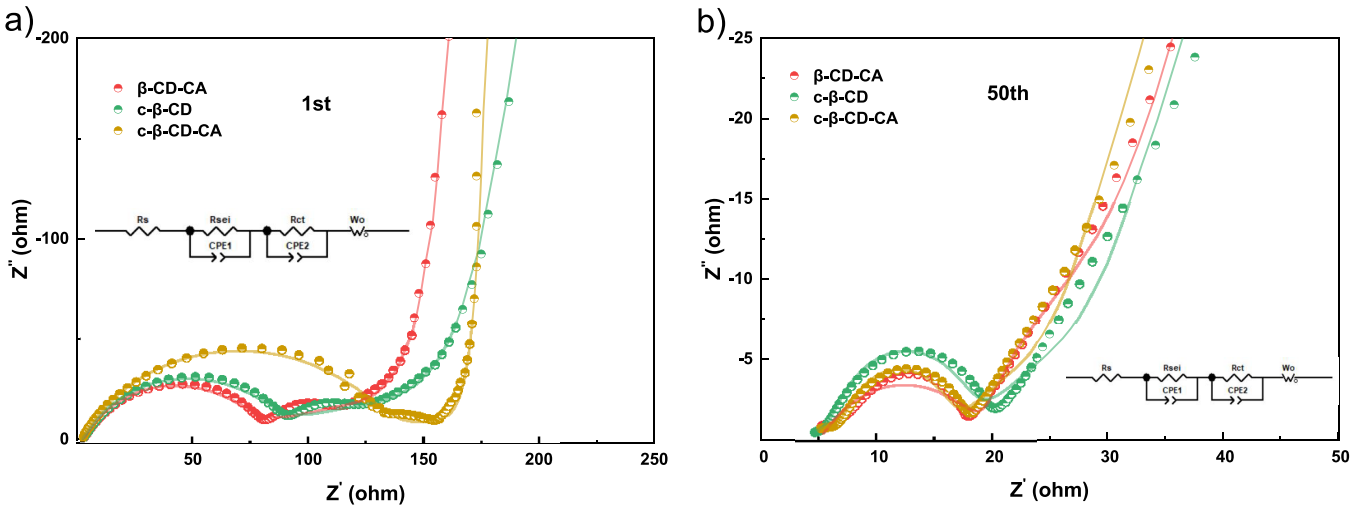

Figure 10. (a) Impedance spectrum after the first cycle. (b) Impedance spectrum after 50 cycles.

Table 1. EIS Fitting Data

sample and cycle numbers		R_s (n)	R_{sei} (0)	R_{ct} (0)
β-CD-CA	1st cycle	1.783	99.76	85.09
	50th cycle	5.228	14.44	9.292
c-β-CD	1st cycle	1.614	75.58	127.9
	50th cycle	4.112	10.53	2.497
c-β-CD-CA	1st cycle	1.773	128.3	51.16
	50th cycle	3.98	7.535	8.219

reversible intermolecular hydrogen bonding produced by the carboxyl group enriched in c-β-CD-CA, which repairs the cracks generated in the lithium-ion embedding-detachment process through the fracture-recombination process. Therefore, the three-dimensional structure of c-β-CD-CA in the integrated electrode prevents Si from falling off the copper foil by the stress and avoids crack generation.

The morphology derived from the local enlargement of each electrode is shown in Figure 12. The spherical morphology of Si is distinctly visible for each electrode before cycling and is uniformly dispersed throughout the pole piece (e.g., Figure 12a−c). The electrode morphologies show remarkable differences after 50 cycles. Among them, the Si particles on the Si/c-β-CD electrode in Figure 12e have been covered by a thick SEI layer. It means the inability of c-β-CD to control the volumetric change of Si particles. In addition, the excessive formation of SEI layers consumes a substantial amount of electrolyte, making it one of the factors for the decline of capacity in subsequent cycles. Compared with the Si/c-β-CD electrode, the cross-linked Si/β-CD-CA electrode in Figure 12d can still clearly distinguish the morphology of individual Si particles even after 50 cycles. It demonstrates that the cross-linked network can more effectively alleviate the volume expansion and yield a relatively stable SEI layer. The Si/c-β-CD-CA electrode not merely inherits the advantages of the cross-linked binder but can also better avoid the particles' agglomeration. The morphology of the 50 cycles is comparable to that before cycling (Figure 12f. It suggests that the c-β-CD-CA in the integrated electrode can well buffer the volume expansion of the encapsulated Si particles.

The cross-sectional thickness provides better visualization of the role of the binder in controlling the Si volume change, as can be seen in Figure 13. The cross-sectional SEM comparison image is in accordance with the trend reflected by the planar SEM, and there are just a small number of cracks in the Si/β-CD-CA electrode in Figure 13a. The Si/c-β-CD-CA electrode in Figure 13c has no apparent crack generation except for some pore structures. In contrast, the Si/c-β-CD electrode in Figure 13b appears to have severe cracks and even powder shedding. The thicknesses of the three electrodes after cycling are 26.0, 31.2, and 20.6 μm. In terms of thickness, the cross-linked

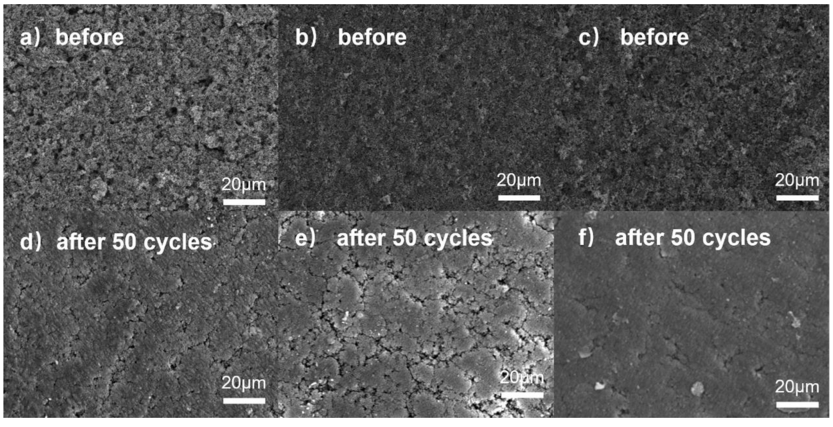

Figure 11. (a, d) Si/β-CD-CA, (b, e) Si/c-β-CD, and (c, f) Si/c-β-CD-CA SEM images of electrodes before and after 50 cycles.

https://doi.org/10.1021/acsomega.2c07182
ACS Omega 2023, 8, 5683−5691

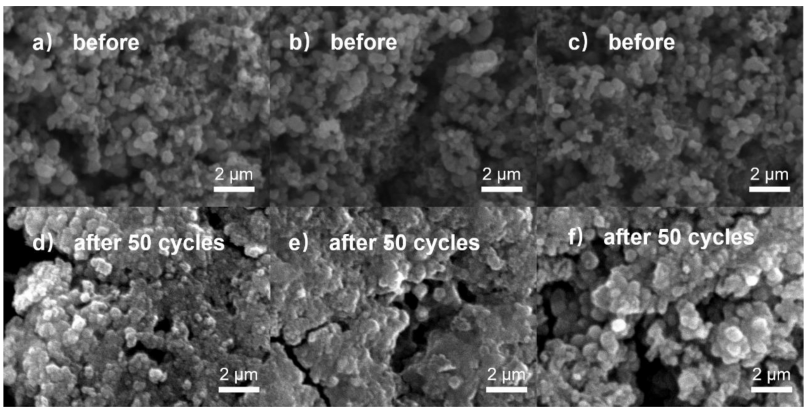

Figure 12. (a, d) Si/β-CD-CA, (b, e) Si/c-β-CD, and (c, f) Si/c-β-CD-CA before and after 50 cycles of scan magnification.

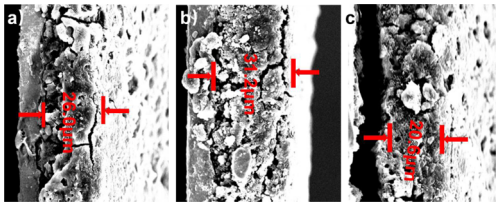

Figure 13. (a) Si/β-CD-CA, (b) Si/c-β-CD, and (c) Si/c-β-CD-CA SEM of cross section of electrode after cycling.

binders β-CD-CA and c-β-CD-CA can significantly mitigate the volume change of Si particles, while the low-molecular-weight c-β-CD cannot effectively control the growth of thickness. These results again indicate that the cross-linked binder is better equipped to buffer the volume change of Si and maintain the structural integrity of the electrode sheet during electrochemical cycling, as well as to mitigate the formation of SEI layers.

4. CONCLUSIONS

In conclusion, we successfully prepared the integrated Si-based electrodes by in situ thermal cross-linking. The electrode is simple to prepare and effectively solves the current Si anode material's volume expansion. The Si/c-β-CD-CA maintains an improved specific capacity of 1941 mAh·g^{-1} after 200 cycles at a high current of 0.5 C. After introducing carboxyl groups, c-β-CD can form lipid-like bonds with the functional groups on the Si surface. The integrated electrode can significantly adapt to Si's volume change and mitigate the formation of a SEI because of lipid-like bonds. Furthermore, the abundant hydrogen bonds in c-β-CD-CA can also self-heal the cracks generated by the electrode in the process of cycling, which effectively preserves the integrity of the integrated electrode. As a result, the Si integrated electrode prepared by in situ cross-linking technology provides a promising application.

■ ASSOCIATED CONTENT

Supporting Information

The Supporting Information is available free of charge at https://pubs.acs.org/doi/10.1021/acsomega.2c07182.

180° peeling test of electrodes, average peeling force of electrodes, CV curves of binders, cycle performance, and rate performance (PDF)

■ AUTHOR INFORMATION

Corresponding Author

Jing Su − *School of Chemistry and Chemical Engineering, Guangxi University, Nanning, Guangxi 530004, China*; Email: sujing@gxu.edu.cn

Authors

Hao-wen Jiang − *School of Chemistry and Chemical Engineering, Guangxi University, Nanning, Guangxi 530004, China*

Yu Qin − *School of Chemistry and Chemical Engineering, Guangxi University, Nanning, Guangxi 530004, China*; orcid.org/0000-0002-5356-6468

Yi-ming Nie − *School of Chemistry and Chemical Engineering, Guangxi University, Nanning, Guangxi 530004, China*

Zhi-fang Su − *School of Chemistry and Chemical Engineering, Guangxi University, Nanning, Guangxi 530004, China*

Yun-fei Long − *School of Chemistry and Chemical Engineering, Guangxi University, Nanning, Guangxi 530004, China*

Yanxuan Wen − *School of Chemistry and Chemical Engineering, Guangxi University, Nanning, Guangxi 530004, China; Guangxi Key Laboratory of Processing for Non-ferrous Metallic and Featured Materials, Guangxi University, Nanning 530004, China*; orcid.org/0000-0003-4712-1953

Complete contact information is available at: https://pubs.acs.org/10.1021/acsomega.2c07182

Author Contributions

[§]H.J. and Y.Q. contributed equally to this work.

Notes

The authors declare no competing financial interest.

■ ACKNOWLEDGMENTS

The authors appreciate the financial support from the Guangxi Natural Science Foundation (No. 2021GXNSFAA220115) and the National Natural Science Foundation of China (No. 51864005).

■ REFERENCES

(1) Fan, L.; Hu, Y. Y.; Rao, A. M.; Zhou, J.; Hou, Z. H.; Wang, C. X.; Lu, B. A. Prospects of Electrode Materials and Electrolytes for Practical Potassium-Based Batteries. *Small Methods* **2021**, *5*, No. 2101131.

(2) Yang, Y. J.; Wu, S. X.; Zhang, Y. P.; Liu, C. B.; Wei, X. J.; Luo, D.; Lin, Z. Towards efficient binders for silicon based lithium-ion battery anodes. *Chem. Eng. J.* **2021**, *406*, No. 126807.
(3) Zuo, X.; Zhu, J.; Mueller-Buschbaum, P.; Cheng, Y. Silicon based lithium-ion battery anodes: A chronicle perspective review. *Nano Energy* **2017**, *31*, 113−143.
(4) Hu, Y. Y.; Fan, L.; Rao, A. M.; Yu, W. J.; Zhuoma, C. X.; Feng, Y. H.; Qin, Z. H.; Zhou, J.; Lu, B. A. Cyclic-anion salt for high-voltage stable potassium-metal batteries. *Natl. Sci. Rev.* **2022**, *9*, nwac134.
(5) Li, S.; Liu, Y.; Zhang, Y.; Song, Y.; Wang, G.; Liu, Y.; Wu, Z.; Zhong, B.; Zhong, Y.; Guo, X. A review of rational design and investigation of binders applied in silicon-based anodes for lithium-ion batteries. *J. Power Sources* **2021**, *485*, No. 229331.
(6) Zhao, Y.; Yue, F.; Li, S.; Zhang, Y.; Tian, Z.; Xu, Q.; Xin, S.; Guo, Y. Advances of polymer binders for silicon-based anodes in high energy density lithium-ion batteries. *InfoMat* **2021**, *3*, 460−501.
(7) Kwon, T.; Choi, J. W.; Coskun, A. The emerging era of supramolecular polymeric binders in silicon anodes. *Chem. Soc. Rev.* **2018**, *47*, 2145−2164.
(8) Peng, L.; Ye, C.; Tong, Q.; Weng, J. Research Progress of Replacing Traditional PVDF Binder with Functional Binder for Lithium Batteries. *Mater. Rep.* **2021**, *35*, 5174−5180.
(9) Yan, L. L.; Gao, X. G.; Wahid-Pedro, F.; Quinn, J.; Meng, Y. Z.; Li, Y. N. A novel epoxy resin-based cathode binder for low cost, long cycling life, and high-energy lithium-sulfur batteries. *J. Mater. Chem. A* **2018**, *6*, 14315−14323.
(10) Lee, S. H.; Lee, J. H.; Nam, D. H.; Cho, M.; Kim, J.; Chanthad, C.; Lee, Y. Epoxidized Natural Rubber/Chitosan Network Binder for Silicon Anode in Lithium-Ion Battery. *ACS Appl. Mater. Interfaces* **2018**, *10*, 16449−16457.
(11) Cano, Z. P.; Banham, D.; Ye, S. Y.; Hintennach, A.; Lu, J.; Fowler, M.; Chen, Z. W. Batteries and fuel cells for emerging electric vehicle markets. *Nat. Energy* **2018**, *3*, 279−289.
(12) Gu, Y. Y.; Yang, S. M.; Zhu, G. B.; Yuan, Y. N.; Qu, Q. T.; Wang, Y.; Zheng, H. H. The effects of cross-linking cations on the electrochemical behavior of silicon anodes with alginate binder. *Electrochim. Acta* **2018**, *269*, 405−414.
(13) Yue, L.; Zhang, L.; Zhong, H. Carboxymethyl chitosan: A new water soluble binder for Si anode of Li-ion batteries. *J. Power Sources* **2014**, *247*, 327−331.
(14) Lestrie, B.; Bahri, S.; Sandu, I.; Roue, L.; Guyomard, D. On the binding mechanism of CMC in Si negative electrodes for Li-ion batteries. *Electrochem. Commun.* **2007**, *9*, 2801−2806.
(15) Komaba, S.; Shimomura, K.; Yabuuchi, N.; Ozeki, T.; Yui, H.; Konno, K. Study on Polymer Binders for High-Capacity SiO Negative Electrode of Li-Ion Batteries. *J. Phys. Chem. C* **2011**, *115*, 13487−13495.
(16) Kovalenko, I.; Zdyrko, B.; Magasinski, A.; Hertzberg, B.; Milicev, Z.; Burtovyy, R.; Luzinov, I.; Yushin, G. A Major Constituent of Brown Algae for Use in High-Capacity Li-Ion Batteries. *Science* **2011**, *334*, 75−79.
(17) Li, Z. H.; Tang, W. T.; Yang, Y. J.; Lai, G. Y.; Lin, Z.; Xiao, H. Y.; Qiu, J. C.; Wei, X. J.; Wu, S. X.; Lin, Z. Engineering Prelithiation of Polyacrylic Acid Binder: A Universal Strategy to Boost Initial Coulombic Efficiency for High-Areal-Capacity Si-Based Anodes. *Adv. Funct. Mater.* **2022**, *32*, No. 2206615.
(18) Wu, S. X.; Yang, Y. J.; Liu, C. B.; Liu, T. F.; Zhang, Y. P.; Zhang, B. K.; Luo, D.; Pan, F.; Lin, Z. In-Situ Polymerized Binder: A Three-in-One Design Strategy for All-Integrated SiOx Anode with High Mass Loading in Lithium Ion Batteries. *ACS Energy Lett.* **2021**, *6*, 290−297.
(19) Choi, S.; Kwon, T.; Coskun, A.; Choi, J. W. Highly elastic binders integrating polyrotaxanes for silicon microparticle anodes in lithium ion batteries. *Science* **2017**, *357*, 279−283.
(20) Sripad, S.; Viswanathan, V. Performance Metrics Required of Next-Generation Batteries to Make a Practical Electric Semi Truck. *ACS Energy Lett.* **2017**, *2*, 1669−1673.
(21) Pang, Q.; Liang, X.; Kwok, C. Y.; Kulisch, J.; Nazar, L. F. A Comprehensive Approach toward Stable Lithium-Sulfur Batteries with High Volumetric Energy Density. *Adv. Energy Mater.* **2017**, *7*, No. 1601630.
(22) Londhe, B. S.; Pratap, U. R.; Mali, J. R.; Mane, R. A. Synthesis of 2-Arylbenzothiazoles Catalyzed by Biomimetic Catalyst, beta-Cyclodextrin. *Bull. Korean Chem. Soc.* **2010**, *31*, 2329−2332.
(23) Jeong, Y. K.; Kwon, T.; Lee, I.; Kim, T.; Coskun, A.; Choi, J. W. Hyperbranched β-cyclodextrin polymer as an effective multidimensional binder for silicon anodes in lithium rechargeable batteries. *Nano Lett.* **2014**, *14*, 864−870.
(24) Zhou, Y.; Zhang, R.; Chen, K.; Zhao, X.; Gu, X.; Lu, J. Enhanced adsorption and photo-degradation of bisphenol A by β-cyclodextrin modified pine sawdust in an aquatic environment. *J. Taiwan Inst. Chem. Eng.* **2017**, *78*, 510−516.
(25) Zhao, F.; Repo, E.; Yin, D.; Meng, Y.; Jafari, S.; Sillanpä, M. EDTA-cross-linked β-cyclodextrin: an environmentally friendly bifunctional adsorbent for simultaneous adsorption of metals and cationic dyes. *Environ. Sci. Technol.* **2015**, *49*, 10570−10580.
(26) Yang, F.; Zhang, B.; Ma, Q. Study of Sticky Rice-Lime Mortar Technology for the Restoration of Historical Masonry Construction. *Acc. Chem. Res.* **2010**, *43*, 936−944.
(27) Wang, J.; Yao, Z.; Monroe, C. W.; Yang, J.; Nuli, Y. Carbonyl-β-cyclodextrin as a novel binder for sulfur composite cathodes in rechargeable lithium batteries. *Adv. Funct. Mater.* **2013**, *23*, 1194−1201.
(28) Wang, Y.; Xu, H.; Chen, X.; Jin, H.; Wang, J. Novel constructive self-healing binder for silicon anodes with high mass loading in lithium-ion batteries. *Energy Storage Mater.* **2021**, *38*, 121−129.
(29) Hamed, A.; Orabi, A.; Salem, H.; Ismaiel, D.; Saad, G.; Abdelhamid, I.; Elwahy, A.; Elsabee, M. An effective uranium removal using diversified synthesized cross-linked chitosan bis-aldehyde Schiff base derivatives from aqueous solutions. *Environ. Sci. Pollut. Res.* **2022**, DOI: 10.1007/s11356-022-23856-2.
(30) Chen, S.; Ling, H. Y.; Chen, H.; Zhang, S.; Du, A.; Yan, C. Development of cross-linked dextrin as aqueous binders for silicon based anodes. *J. Power Sources* **2020**, *450*, No. 227671.
(31) Cao, P. F.; Yang, G.; Li, B. R.; Zhang, Y. M.; Zhao, S.; Zhang, S.; Erwin, A.; Zhang, Z. C.; Sokolov, A. P.; Nanda, J.; Saito, T. Rational Design of a Multifunctional Binder for High-Capacity Silicon-Based Anodes. *ACS Energy Lett.* **2019**, *4*, 1171−1180.
(32) Vogl, U. S.; Das, P. K.; Weber, A. Z.; Winter, M.; Kostecki, R.; Lux, S. F. Mechanism of Interactions between CMC Binder and Si Single Crystal Facets. *Langmuir* **2014**, *30*, 10299−10307.
(33) Shen, L. Y.; Shen, L.; Wang, Z. X.; Chen, L. Q. In Situ Thermally Cross-linked Polyacrylonitrile as Binder for High-Performance Silicon as Lithium Ion Battery Anode. *ChemSusChem* **2014**, *7*, 1951−1956.
(34) Chuang, Y.; Lin, Y.; Wang, C.; Hong, J. Dual Cross-Linked Polymer Networks Derived from the Hyperbranched Poly(ethyleneimine) and Poly(acrylic acid) as Efficient Binders for Silicon Anodes in Lithium-Ion Batteries. *ACS Appl. Energy Mater.* **2021**, *4*, 1583−1592.
(35) Chen, Z.; Zhang, H.; Dong, T.; Mu, P.; Rong, X.; Li, Z. Uncovering the Chemistry of Cross-Linked Polymer Binders via Chemical Bonds for Silicon-Based Electrodes. *ACS Appl. Mater. Interfaces* **2020**, *12*, 47164−47180.
(36) Zhao, Y.; Yue, F.; Li, S.; Zhang, Y.; Tian, Z.; Xu, Q.; Xin, S.; Guo, Y. Advances of polymer binders for silicon-based anodes in high energy density lithium-ion batteries. *InfoMat* **2021**, *3*, 460−501.

https://doi.org/10.1021/acsomega.2c07182
ACS Omega 2023, 8, 5683−5691